

Bifurcation and spectral entropy complexity of a fractional-order SVIRS epidemic system

Zhen Wang^a, Gongsheng Li^{b,*}, Pingping Li^b

^a College of Science, Inner Mongolia University of Technology, Hohhot, Inner Mongolia 010100 China

^b School of Mathematics and Statistics, Shandong University of Technology, Zibo, Shandong 255000 China

*Corresponding author, e-mail: ligs@sdut.edu.cn

Received 6 Jun 2025, Accepted 2 Mar 2026

Available online

ABSTRACT: This article deals with bifurcation dynamics and complexity of a nonlinear fractional-order SVIRS epidemic system. Based on the analysis of the disease-free and endemic equilibriums, the forward (supercritical) and backward (subcritical) bifurcations are observed around the basic reproduction number. The complexity of the fractional epidemic system is estimated by spectral entropy and numerical simulations, and the relation of the order of the fractional derivative with dynamics of the system is investigated and illustrated by the complexity. The spectral entropy complexity can be regarded as an index to connect oscillatory bifurcations with the order of the fractional derivative for the fractional-order epidemic system.

KEYWORDS: time-fractional epidemic system, dynamics, bifurcation, spectral entropy, numerical simulation

MSC2020: 34A08 92C45

INTRODUCTION

Compartment models are typically employed to simulate a wide variety of phenomena, including epidemics, in-host pathogen dynamics, and pharmacokinetics of active substances in the human body, etc. In a standard compartment model the populations or concentrations of species evolved through a set of coupled ordinary differential equations (ODEs), where the model assumes that each compartment is well mixed with a homogeneous population. This leads to traditional infectious disease dynamic systems. For example, Anderson et al [1] analyzed the biology of infectious diseases in populations, Hethcote explained the mathematical theory underlying epidemics [2], and Ma et al [3] studied mathematical modeling and analytical methods for infectious diseases in the monograph.

With the research advancement on fractional calculus, fractional dynamics and anomalous diffusion in recent decades, there has been a significant interest in the study of nonlocal epidemic dynamics models incorporating fractional derivatives. For example, the diffusion of drugs in a human organ system was simulated by a fractional compartmental model [4], the transmission of infectious diseases such as dengue [5], H1N1 [6] and HIV/AIDS [7, 8] was studied by utilizing fractional derivative models, a general framework for time fractional-order compartment models was proposed [9, 10], and spatial dynamics of a nonlocal epidemic model was explored [11], etc. With the outbreak of COVID-19, there has been a surge in research on the model construction, numerical simulation and prediction of the epidemic with a large number of fractional-order dynamical systems. Ahmad et al [12] investigated COVID-19 transmission within fractional-

order infectious disease models; Boudaoui et al [13] analyzed the spread dynamics using fractional models with nonsingular kernels; Ghori et al [14] examined global dynamics and bifurcation behaviors in fractional SEIR models; Higazy et al [15] proposed a new fractional-order mathematical model to describe the transmission of COVID-19; Pandey et al [16] studied a novel fractional model of COVID-19 epidemic considering quarantine and latent time. Recently, Lu et al [17] studied an anomalous diffusion epidemic model based on random walks and distributed delays; Wu et al [18] analyzed global stability of fractional SIS models; Wang and Li investigated chaos phenomena depending upon differentiation orders in a fractional SAIR model [19]; Nisar et al [20] gave a review for life-science challenges in fractional-order epidemic frameworks.

It is noted that the vaccinations are beneficial to the prevention and control of infectious diseases [21, 22], however, a vaccinated person could be infected and become a sufferer with infectivity, and a recovered person could not have permanent immunity, i.e., some recovered peoples can lose the immunity and become the susceptible. Henceforth, we consider a fractional-order SVIRS (*S*: Susceptible, *V*: Vaccinated; *I*: Infectious; *R*: Recovered) epidemic system in this paper, which is given as:

$$\begin{cases} {}_0^C D_t^\alpha S(t) = \Lambda - \beta S(t)I(t) + \mu R(t) - (\eta + d)S(t), \\ {}_0^C D_t^\alpha V(t) = \eta S(t) - \beta_1 V(t)I(t) - dV(t), \\ {}_0^C D_t^\alpha I(t) = \beta S(t)I(t) + \beta_1 V(t)I(t) - (\gamma + d)I(t), \\ {}_0^C D_t^\alpha R(t) = \gamma I(t) - (\mu + d)R(t), \end{cases} \quad (1)$$

where $S(t), V(t), I(t), R(t)$ denote the number of the susceptible, the vaccinated, the infectious and the

recovered people respectively; ${}_0^C D_t^\alpha f(t)$ denotes the Caputo derivative of a function $f(t)$ on $t > 0$, which is defined by [23]

$${}_0^C D_t^\alpha f(t) = \frac{1}{\Gamma(1-\alpha)} \int_0^t (t-\tau)^{-\alpha} f'(\tau) d\tau, \quad t > 0, \quad (2)$$

here $\alpha \in (0, 1)$ is the fractional order; Λ is the immigration rate, β and β_1 are the contact rates between the susceptible, the vaccinated and the infectious persons respectively, μ is the immunity loss rate, η is the vaccination rate, d is the mortality rate, and γ is the recovery rate. All the above parameters are nonnegative constants. The initial values of the system (1) are given as

$$S(0) = S_0; V(0) = V_0; I(0) = I_0; R(0) = 0, \quad (3)$$

where S_0 , V_0 and I_0 are positive constants, and the recovered people at the initial time are assumed to be zero. Thus we get a forward problem composed by the system (1) with the initial condition (3), which is a nonlinear fractional-order dynamics problem.

As we know, the fractional order in a fractional differential equation model serves as a crucial parameter, and it can significantly influence the dynamic behaviors of the fractional system resulting in bifurcations and chaos. So it is very important to estimate and quantify the effectiveness of the fractional order in a fractional dynamic system. Nevertheless, there are few studies relatively on dynamic analysis of fractional orders in fractional models, and it is a crucial problem to reveal dynamic process and mechanism of nonlinear fractional system on the order of the fractional derivative. To address this issue, we employ the spectral entropy (SE) complexity algorithm to specifically investigate the role of the order in the fractional system.

In this paper we firstly investigate dynamics of the fractional-order epidemic system based on the basic reproduction number and the center manifold method. By utilizing the modified center manifold method for general system of ODEs [24], we find forward/backward bifurcations of the system on the infection rate around the disease-free equilibrium under suitable conditions of the parameters. In particular, we observe that there occurs backward bifurcation when the basic reproduction number across the critical value of 1, and there exhibits a region of coexistence for the disease-free equilibrium and the endemic equilibria. However, the dynamic bifurcations here seem to have no relations with the order of the fractional derivative, it is still necessary to study the dynamics of the fractional-order epidemic system by other approaches.

It is noted that the SE analysis [25, 26] is an effective method used to analyze complexity of a nonlinear system, which has been widely used in various fields [27, 28]. We will give a structural complexity for

the fractional-order epidemic system on the fractional order by utilizing the SE complexity and numerical simulations. By the SE complexity analysis for the fractional-order epidemic system, we find that there exists a critical index of the fractional order, and the system can occur oscillatory bifurcations when the order is less than the index, which is the main contribution of this paper.

For fractional-order nonlinear dynamic systems, various methods currently exist for obtaining semi-analytical or asymptotic solutions of nonlinear systems, such as the finite difference method for time fractional diffusion equations [29], the quadratic spline collocation method [30], the preconditioning iterative method with graded time steps [31], the fast compact difference scheme with unequal time steps [32], the Adomian decomposition method [33], etc. In this paper we will apply the fractional predictor-corrector method [34, 35], proposed by Kai et al in 2002, to solve the system (1) numerically.

The highlights and findings of this paper are given below:

This paper analyzes the forward/backward bifurcation dynamics of the infectious coefficient near the critical threshold $R_0 = 1$, and the dynamics of the fractional system varying with the order of the fractional derivative. By applying spectral entropy (SE) algorithm, we investigate the relationship between the fractional order and the structural complexity, and thereby to reveal their functional roles in the dynamical system.

DYNAMIC ANALYSIS BASED ON THE BASIC REPRODUCTION NUMBER

The disease-free and endemic equilibriums

Let $I(t) = 0$, and there is $R(t) = 0$. Based on the first and second equations of the system (1), we can obtain $S_0 = \frac{\Lambda}{\eta+d}$ and $V_0 = \frac{\Lambda\eta}{(\eta+d)d}$, respectively. Thus, we get the disease-free equilibrium of the system (1):

$$E_0 = (S_0, V_0, 0, 0). \quad (4)$$

By the concept of basic reproduction number, we define

$$R_0 = \frac{\beta S_0 + \beta_1 V_0}{\gamma + d} = \frac{\Lambda(\beta d + \beta_1 \eta)}{(\gamma + d)(\eta + d)d} \quad (5)$$

as the basic reproduction number of the system (1). Now we consider endemic equilibrium of the system (1).

By setting the right-hand sides of all equations in system (1) be zero, we obtain:

$$\begin{cases} \Lambda - \beta S(t)I(t) + \mu R(t) - (\eta + d)S(t) = 0 \\ \eta S(t) - \beta_1 V(t)I(t) - dV(t) = 0 \\ \beta S(t) + \beta_1 V(t) - (\gamma + d) = 0 \\ \gamma I(t) - \mu R(t) - dR(t) = 0 \end{cases} \quad (6)$$

By the second and fourth equations of the Eq. (6), we have

$$V = \frac{\eta}{\beta_1 I + d} S, \tag{7}$$

and

$$R = \frac{\gamma}{\mu + d} I. \tag{8}$$

By substituting Eq. (7) into the third equation of (6), we get

$$S = \frac{(\gamma + d)(\beta_1 I + d)}{(\beta_1 I + d)\beta + \beta_1 \eta}. \tag{9}$$

Then by substituting Eq. (8) and Eq. (9) into the first equation of system (1), we get a quadratic equation of I :

$$a_2 I^2 + a_1 I + a_0 = 0, \tag{10}$$

where

$$\begin{cases} a_2 = \beta \beta_1 (\gamma + d) \left(1 - \frac{\mu \gamma}{(\gamma + d)(\mu + d)}\right), \\ a_1 = k_1 (R_0 - R_1), \\ a_0 = d(\eta + d)(\gamma + d)(1 - R_0), \end{cases} \tag{11}$$

and

$$\begin{cases} k_1 = \frac{(\gamma + d)^2 (\eta + d) d}{\Lambda} \left(1 - \frac{\mu \gamma}{(\gamma + d)(\mu + d)}\right), \\ R_1 = \frac{(\mu + d)(\Lambda \beta - (\gamma + d)d) \beta_1}{(\mu + d)(\gamma + d) - \mu \gamma} \frac{\Lambda}{(\gamma + d)(\eta + d)d}. \end{cases} \tag{12}$$

For Eq. (10), there is

$$\begin{aligned} \Delta &= a_1^2 - 4a_2 a_0 \\ &= k_1^2 (R_0 - R_1)^2 - 4\beta \beta_1 d (\gamma + d)^2 \\ &\quad \times (\eta + d) \left(1 - \frac{\mu \gamma}{(\gamma + d)(\mu + d)}\right) (1 - R_0) \\ &= k_1^2 [R_0^2 + (4k_2 - 2R_1)R_0 + R_1^2 - 4k_2] \\ &= k_1^2 (R_0 - r_1)(R_0 - r_2), \end{aligned} \tag{13}$$

where

$$\begin{aligned} r_1 &= R_1 - 2k_2 + 2\sqrt{k_2^2 + k_2(1 - R_1)}, \\ r_2 &= R_1 - 2k_2 - 2\sqrt{k_2^2 + k_2(1 - R_1)}, \end{aligned} \tag{14}$$

and

$$k_2 = \frac{\Lambda^2 \beta \beta_1}{(\gamma + d)^2 (\eta + d)d} \left(1 - \frac{\mu \gamma}{(\gamma + d)(\mu + d)}\right). \tag{15}$$

Thanks to $a_2 > 0$ and $k_1, k_2 > 0$, we deduce that Eq. (10) has two real roots when $R_0 > r_1$ or $R_0 < r_2$. In addition, Eq. (10) has only one real root when $\Delta = 0$, i.e., $R_0 = r_1 > R_1$ or $R_0 = r_2 < R_1$, and it has no real roots when $r_2 < R_0 < r_1$.

Noting that an equilibrium of the system must be positive, so the model parameters can not be chosen arbitrarily, and one condition is that the coefficient a_1 given in (11) should take negative values such that Eq. (10) can have positive solutions. Henceforth, we get the existence results of endemic equilibriums of the system (1) given in the following theorem.

Theorem 1 Assume that all parameters in the system (1) are nonnegative constants, and the coefficients R_1 and k_2 given by (12) and (15) satisfy the condition $R_1 \leq 1 + k_2$, then there hold

- (1) The system (1) have two endemic equilibriums if $R_0 < r_2$, where r_2 is given in (14);
- (2) The system (1) has one endemic equilibrium if $R_0 = r_2$;
- (3) The system (1) has no endemic equilibriums if $R_0 > r_2$.

Forward/backward bifurcations

According to Theorem 1, the dynamical system (1) can have two endemic equilibrium points when the parameters satisfy the condition $R_0 < r_2 < R_1$. This means that the infectious disease may continue to spread even when $R_0 < 1$. So we study the forward/backward bifurcations of the dynamic system on the infection rate around the critical point of $R_0 = 1$ by the modified center manifold method (see Theorem 4.1 and Corollary 4.1 in [24]).

By Eq. (5) and letting $R_0 = 1$, the critical value of the bifurcation parameter is given as

$$\beta^* = \frac{(\gamma + d)(\eta + d)d - \Lambda \beta_1 \eta}{\Lambda d}. \tag{16}$$

Let $x_1 = S, x_2 = V, x_3 = I$ and $x_4 = R$ for convenience of writing, and the system (1) can be written as $\partial_t^\alpha \mathbf{x} = \mathbf{f}(\mathbf{x}, \beta^*)$, where $\mathbf{x} = (x_1, x_2, x_3, x_4)$, and $\mathbf{f} = (f_1, f_2, f_3, f_4)$ where $f_n, n = 1, 2, 3, 4$, denote the right-hand terms of the system (1) respectively. On forward and backward bifurcations of a dynamic system, the following lemma gives a criteria.

Lemma 1 ([24]) Let $\mathbf{f}(E_0, \beta^*) = 0, \mathbf{A} = (\frac{\partial f_n}{\partial x_i}) (n = 1, \dots, 4, i = 1, \dots, 4)$ is the Jacobian matrix of the dynamic system at the point (E_0, β^*) . If zero is a simple eigenvalue of the matrix \mathbf{A} , and all other eigenvalues have negative real parts, and h and l are the left and right eigenvectors corresponding to the zero eigenvalue, where the vector l takes nonnegative values. Then there occurs backward bifurcation when $a, b > 0$, and it occurs forward bifurcation when $a < 0$ and $b > 0$, where

$$\begin{aligned} a &= \sum_{n,i,j=1}^4 l_n h_i h_j \frac{\partial^2 f_n}{\partial x_i \partial x_j} \Big|_{\mathbf{x}=E_0, \beta=\beta^*}, \\ b &= \sum_{n,i=1}^4 l_n h_i \frac{\partial^2 f_n}{\partial x_i \partial \beta} \Big|_{\mathbf{x}=E_0, \beta=\beta^*}. \end{aligned} \tag{17}$$

By this lemma we can determine the direction of the bifurcation of the system (1) at $R_0 = 1$.

Theorem 2 Denote

$$r_3 = \frac{\eta}{4(\eta + d)} + \frac{\mu \gamma}{(\mu + d)(\gamma + d)}. \tag{18}$$

Assume that all the parameters are nonnegative constants, and the mortality rate d is suitably small, and $r_3 \geq 1$ holds, then we have

- (1) The system (1) has backward bifurcation at $R_0 = 1$ if $\beta_{11} < \beta_1 < \beta_{12}$;
- (2) The system (1) has forward bifurcation at $R_0 = 1$ if $\beta_1 < \beta_{11}$ or $\beta_1 > \beta_{12}$, where β_{11} and β_{12} are given by Eq. (26) in the proof.

Proof: By substituting $\beta^* = \beta$ into the Jacobian matrix, we have

$$J(E_0, \beta^*) = \begin{pmatrix} -\eta - d & 0 & -\beta^* S_0 & \mu \\ \eta & -d & -\beta_1 V_0 & 0 \\ 0 & 0 & 0 & 0 \\ 0 & 0 & \gamma & -\mu - d \end{pmatrix} \quad (19)$$

and the characteristic equation of (19) is

$$\lambda(\lambda + d)(\lambda + \eta + d)(\lambda + \mu + d) = 0.$$

It can be seen that the Jacobian matrix (19) has only one zero eigenvalue, and the other eigenvalues are negative. In what follows we estimate the sign of the coefficients a and b given by Eq. (17) in Lemma 1.

Let $h = (h_1, h_2, h_3, h_4)^T$ and $l = (l_1, l_2, l_3, l_4)$ be the right and left eigenvectors corresponding to the eigenvalue of zero, respectively. By computation we have

$$\begin{cases} h_1 = \frac{\mu\gamma}{(\mu+d)(\eta+d)} - \frac{\beta^* S_0}{(\eta+d)}, \\ h_2 = \frac{\eta\mu\gamma}{(\mu+d)(\eta+d)d} - \frac{\eta\beta^* S_0}{(\eta+d)d} - \frac{\beta_1 V_0}{d}, \\ h_3 = 1, \\ h_4 = \frac{\gamma}{\mu+d}, \end{cases} \quad (20)$$

and

$$l_1 = 0, \quad l_2 = 0, \quad l_3 = 1, \quad l_4 = 0.$$

Then by Eq. (17) in Lemma 1, we get

$$\begin{aligned} a &= 2l_3 \left(h_1 h_3 \frac{\partial^2 f_3}{\partial x_1 \partial x_3} + h_2 h_3 \frac{\partial^2 f_2}{\partial x_2 \partial x_3} \right)_{x=E_0, \beta=\beta^*} \\ &= 2l_3 h_3 (h_1 \beta^* + h_2 \beta_1) \\ &= 2(h_1 \beta^* + h_2 \beta_1) \end{aligned} \quad (21)$$

and

$$b = l_3 h_3 \left(\frac{\partial^2 f_2}{\partial x_3 \partial \beta^*} \right)_{x=E_0, \beta=\beta^*} = h_3 S^0 = \frac{\Lambda(\mu + d)}{\gamma(\eta + d)}. \quad (22)$$

It is obvious that $b > 0$ holds, and we need to determine the sign of a . By Eq. (20) we have

$$\begin{aligned} h_1 \beta^* + h_2 \beta_1 &= -\frac{\Lambda\eta}{(\eta+d)d^2} \beta_1^2 + \frac{\eta(\gamma+d)}{(\eta+d)d} \beta_1 \\ &\quad + \frac{\gamma+d}{\Lambda} \left[\frac{\mu\gamma}{\mu+d} - (\gamma+d) \right] \\ &= c_2 \beta_1^2 + c_1 \beta_1 + c_0, \end{aligned} \quad (23)$$

where

$$\begin{cases} c_2 = -\frac{\Lambda\eta}{(\eta+d)d^2}, \\ c_1 = \frac{\eta(\gamma+d)}{(\eta+d)d}, \\ c_0 = \frac{\gamma+d}{\Lambda} \left[\frac{\mu\gamma}{\mu+d} - (\gamma+d) \right]. \end{cases} \quad (24)$$

Denote $F(\beta_1) = c_2 \beta_1^2 + c_1 \beta_1 + c_0$. Since

$$\begin{aligned} \Delta_2 &= c_1^2 - 4c_2 c_0 \\ &= \frac{\eta^2(\gamma+d)^2}{(\eta+d)^2 d^2} + 4 \frac{(\gamma+d)\eta}{(\eta+d)d^2} \left(\frac{\mu\gamma}{\mu+d} - (\gamma+d) \right) \\ &= 4 \frac{(\gamma+d)^2 \eta}{(\eta+d)d^2} \left(\frac{\eta}{4(\eta+d)} + \frac{\mu\gamma}{(\mu+d)(\gamma+d)} - 1 \right) \\ &= 4 \frac{(\gamma+d)^2 \eta}{(\eta+d)d^2} (r_3 - 1), \end{aligned} \quad (25)$$

and thanks to $r_3 \geq 1$, there exist real solutions to the equation $F(\beta_1) = 0$, which are expressed by

$$\beta_{11} = \frac{c_1 - \sqrt{\Delta_2}}{-2c_2}, \quad \beta_{12} = \frac{c_1 + \sqrt{\Delta_2}}{-2c_2}. \quad (26)$$

Noting $c_2 < 0$, $c_1 > \sqrt{\Delta_2} \geq 0$, there is $0 < \beta_{11} \leq \beta_{12}$. By the properties of the quadratic function, there must have $F(\beta_1) > 0$ if there holds $\beta_{11} < \beta_1 < \beta_{12}$, and then we get $a = 2F(\beta_1) > 0$. Together with $b > 0$ follows that there occurs backward bifurcation by Lemma 1. Otherwise, we get $a < 0$ if there holds $\beta_1 < \beta_{11}$, or $\beta_1 > \beta_{12}$, and forward bifurcation occurs. \square

Remark 1 The condition $r_3 \geq 1$ is not strict to the parameters if the mortality rate d is small enough. In fact, there holds $\lim_{d \rightarrow 0} r_3 = 5/4$. So the condition holds in general cases as long as the mortality rate is suitably small.

In what follows we give two examples to illustrate the forward/backward bifurcations based on the theoretical analysis.

Example 1 Take the parameters as: $\Lambda = 1$, $\gamma = 0.5$, $\eta = 0.25$, $\mu = 0.4$ and $d = 0.025$. By Eq. (25) and Eq. (26) we get $\Delta_2 = 198.2596$, and $\beta_{11} = 0.0017$, $\beta_{12} = 0.0114$.

Let $\beta_1 = 0.001$. There holds $\beta_1 < 0.0017 = \beta_{11}$, and there must occur forward bifurcation at $R_0 = 1$ according to the assertion (2) of Theorem 2. We plot the solution I with the basic reproduction number R_0 in Fig. 1(a). It can be seen that the forward bifurcation occurs around $R_0 = 1$, which indicates that the disease-free equilibrium is stable when $R_0 < 1$, but the system can admit a stable endemic equilibrium as R_0 across the critical point.

Similarly, let $\beta_1 = 0.012$, and there is $\beta_1 > 0.0114 = \beta_{12}$, and the assertion (2) of Theorem 2 is also valid. As observed in Fig. 1(b), the dynamic system occurs the forward bifurcation around $R_0 = 1$ again.

Example 2 Let $\beta_1 = 0.005$, and the other parameters are the same as used in Example 1. At this time the

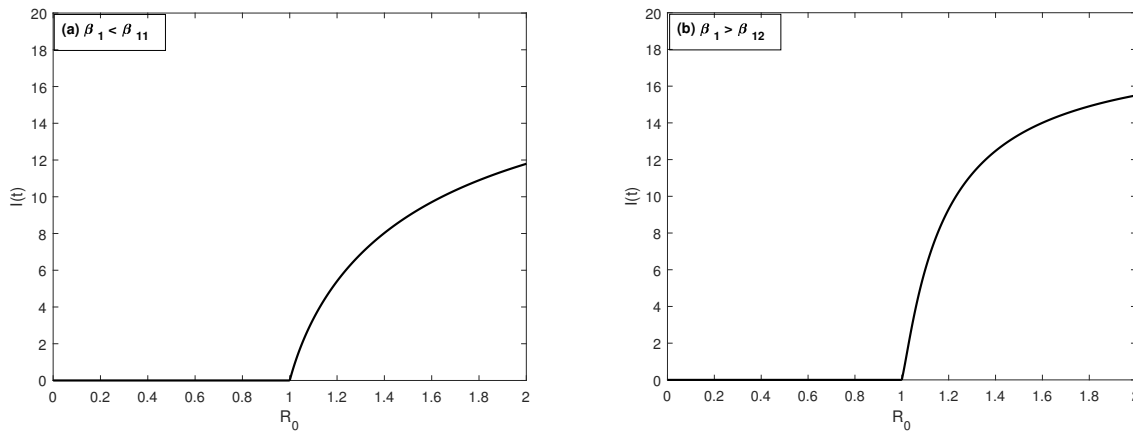


Fig. 1 Forward bifurcations at $R_0 = 1$ in Example 1.

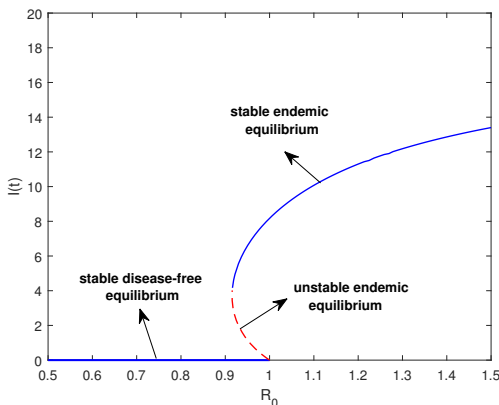


Fig. 2 Backward bifurcation at $R_0 = 1$ in Example 2.

assertion (1) of Theorem 2 is valid due to $\beta_{11} < \beta_1 < \beta_{12}$, and there occurs the backward bifurcation at $R_0 = 1$, which is plotted in Fig. 2.

From this illustration it can be seen that the infectious disease could not be eliminated even if $R_0 < 1$ holds, and there exhibits a region of coexistence for the disease-free equilibrium and the endemic equilibria. We also find that a smaller endemic equilibrium, i.e., with a small number of infected individuals, it is unstable, and a larger one, i.e., with a larger number of infected individuals, it is stable.

NUMERICAL SIMULATIONS

In order to observe dynamical behaviors of the system (1) clearly, and to explore the relationship of the dynamics with the fractional orders, we carry out numerical simulations for the system (1) by utilizing the predictor-corrector method [34, 35]. We give the main procedures of this numerical method for the completeness of this paper.

Predictor-corrector method

Consider a nonlinear fractional differential equation for given $T > 0$:

$${}_0^C D_t^\alpha y(t) = f(t, y(t)), \quad t \in (0, T], \quad (27)$$

where $f(\cdot, \cdot)$ is a nonlinear function, and the initial value is known as $y(0) = y_0$.

For given integer number $N > 1$, take a uniform grid $\{t_n = nh : n = 0, 1, \dots, N\}$, where $h = \frac{T}{N}$ is a step size. By the Volterra integral expression for Eq. (27), we have

$$y(t) = y(0) + \frac{1}{\Gamma(\alpha)} \int_0^t (t - \xi)^{\alpha-1} f(\xi, y(\xi)) d\xi. \quad (28)$$

Denote $y_h(t_j) = y(t_j)$, $j = 0, 1, \dots, n$, there is

$$y_h(t_{n+1}) = y(0) + \frac{1}{\Gamma(\alpha)} \int_0^{t_{n+1}} (t_{n+1} - \xi)^{\alpha-1} f(\xi, y(\xi)) d\xi. \quad (29)$$

By using the trapezoidal numerical integration formula, we have

$$y_h(t_{n+1}) = y(0) + \frac{h^\alpha}{\Gamma(\alpha + 2)} f(t_{n+1}, y_h(t_{n+1})) + \frac{h^\alpha}{\Gamma(\alpha + 2)} \sum_{j=0}^n a_{j,n} f(t_j, y_h(t_j)), \quad (30)$$

where

$$a_{j,n} = \begin{cases} n^{\alpha+1} - (n - \alpha)(n + 1)^\alpha, & j = 0, \\ (n - j + 2)^{\alpha+1} + (n - j)^{\alpha+1} - 2(n - j + 1)^{\alpha+1}, & 1 \leq j \leq n. \end{cases}$$

By the predictor-corrector method, the term $y_h(t_{n+1})$ in the right-hand side of Eq. (30) is replaced by an approximation which is given as:

$$y_h(t_{n+1}) \approx y(0) + \frac{1}{\Gamma(\alpha)} \sum_{j=0}^n b_{j,n} f(t_j, y_h(t_j)), \quad (31)$$

where

$$b_{j,n} = \frac{h^\alpha}{\alpha} ((n+1-j)^\alpha - (n-j)^\alpha).$$

So we can work out numerical solutions of $y_h(t_n)$, $n = 1, \dots, N$, layer-by-layer by Eq. (30). This is the predictor-corrector method for solving nonlinear differential equations.

Numerical experiments

In this subsection, we give numerical solutions to the fractional system (1) by using the predictor-corrector method.

Example 3 Let initial values of the system (1) be $S(0) = 100$, $V(0) = 50$, $I(0) = 10$ and $R(0) = 0$, the final time be $T = 100$, and the step size be $h = 0.05$ in the concrete computations. The model parameters are chosen as $\Lambda = 2$, $\beta = 0.07$, $\beta_1 = 0.001$, $\mu = 0.2$, $\eta = 0.4$, $\gamma = 0.6$ and $d = 0.01$.

We firstly take small fractional orders to perform numerical simulations. The numerical solutions with $\alpha = 0.40$ and 0.45 are plotted in Fig. 3(a,b), respectively.

In addition, the solutions with $\alpha = 0.55$, 0.60 , 0.80 , and 0.95 are plotted in Fig. 4(a–d), respectively.

From Figs. 3–4 it can be seen that the fractional order plays an important role in the change of solutions to the dynamic system (1), which can increase the complexity of the system. The system can occur oscillatory bifurcations when using smaller orders less than $\alpha = 0.5$ as observed in Fig. 3, and the solutions of the system become stable when the fractional order takes larger values more than $\alpha = 0.5$ as observed in Fig. 4.

COMPLEXITY AND OSCILLATORY BIFURCATION

By the numerical simulations in Section 3, we can see that the fractional system occurs oscillatory bifurcations if the order of the fractional derivative takes small values. In this section, we devote to giving an explanation to this dynamical behaviors by using a spectral entropy complexity.

In what follows we introduce the SE algorithm [25, 26] for completeness of this paper.

Step 1. Give a sequence $\{x(n), n = 0, 1, \dots, N-1\}$ of length N , where $N > 1$ is an even number, update it by

$$x_n = x(n) - \bar{x}, \quad (32)$$

where $\bar{x} = \frac{1}{N} \sum_{n=0}^{N-1} x(n)$.

Step 2. Perform Fourier transform on the sequence x_n ($n = 0, 1, \dots, N-1$), there holds

$$X(k) = \sum_{n=0}^{N-1} x_n e^{-i \frac{2\pi}{N} nk}, \quad (33)$$

where $k = 0, 1, \dots, N-1$.

Step 3. For the sequence $X(k)$ given by Eq. (33), take the first half to calculate, and work out the power spectrum value of a certain frequency point according to Parseval's theorem:

$$p(k) = |X(k)|^2, \quad (34)$$

where $k = 0, 1, \dots, \frac{N}{2}-1$. The sequence total power is defined as

$$p_{\text{tot}} = \sum_{k=0}^{N/2-1} |X(k)|^2, \quad (35)$$

and the relative power spectrum probability P_k of the sequence is given by

$$P_k = \frac{p(k)}{p_{\text{tot}}} = \frac{|X(k)|^2}{\sum_{k=0}^{N/2-1} |X(k)|^2}. \quad (36)$$

Obviously, there is $\sum_{k=0}^{N/2-1} P_k = 1$. By using the concept of Shannon entropy, define a spectral entropy via

$$SE = - \sum_{k=0}^{N/2-1} P_k \ln P_k, \quad (37)$$

where we set $SE = 0$ if $P_k = 0$.

Step 4. In order to facilitate comparative analysis, the SE is normalized and given as

$$SE(N) = \frac{-1}{\ln(N/2)} \sum_{k=0}^{N/2-1} P_k \ln P_k. \quad (38)$$

For given model parameters and a final time $T > 0$, the system (1) can be solved numerically, and the solutions are obtained, denoted as sequences of S_n , V_n , I_n and R_n for $n = 0, 1, \dots$. In what follows we investigate the complexity and dynamics of the system (1) by calculating the values of SE of the solutions.

Example 4 Let the model parameters be the same as used in Example 3, and work out numerical solutions to the system (1) by Eq. (30) as the corresponding sequences. Noting $T = 100$ and $h = 0.05$, the length of each sequence is $N = 2000$. In order to quantify the effect of the fractional order on the fractional system, we set $\alpha \in [0.3, 1]$, and discrete the interval of orders with $\tau = 0.01$, and work out the SE values of each state variables of the system (1) varying with the orders by the SE algorithm. The computational results are denoted by SE(S), SE(V), SE(I) and SE(R), and plotted in Fig. 5, respectively.

Moreover, denote

$$SE_{\text{Tot}} = \frac{1}{4} [SE(S) + SE(V) + SE(I) + SE(R)], \quad (39)$$

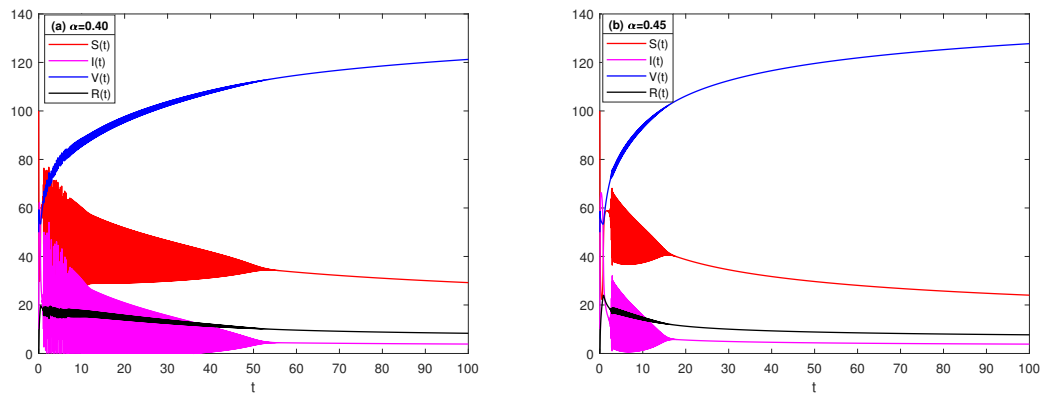


Fig. 3 Numerical solutions with (a) $\alpha = 0.40$ and (b) $\alpha = 0.45$ in Example 3.

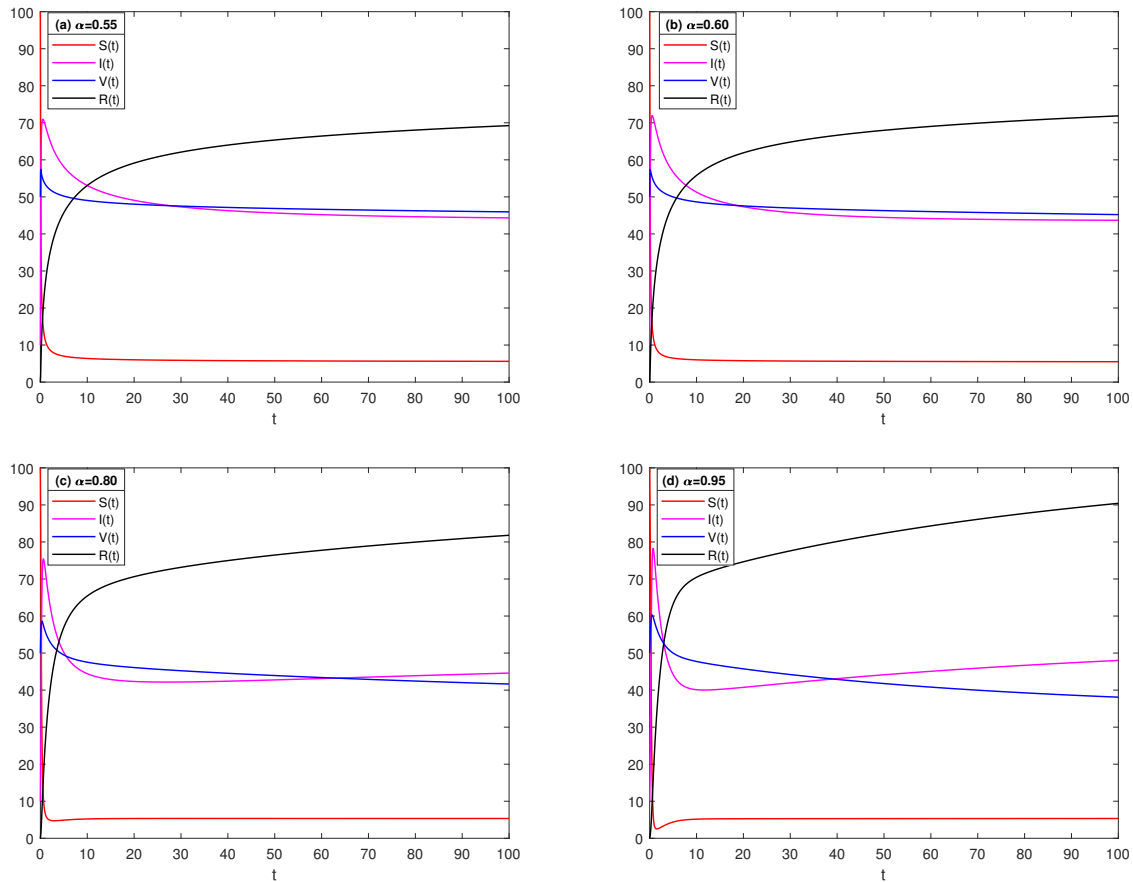


Fig. 4 Numerical solutions with α : (a) 0.55, (b) 0.60, (c) 0.80, and (d) 0.95 in Example 3.

as a total SE value of the fractional system, which is plotted in Fig. 6.

It can be seen from Figs. 5–6 that when $\alpha < 0.5$, the change of SE is relatively drastic, and the dynamic system occurs bifurcation as observed in Fig. 3. When

$\alpha > 0.5$, the SE becomes steady, and there is no bifurcation behaviors in the numerical simulations as observed in Fig. 4.

Although we can not determine why the critical value of the fractional order is about $\alpha^* = 0.5$ in theory,

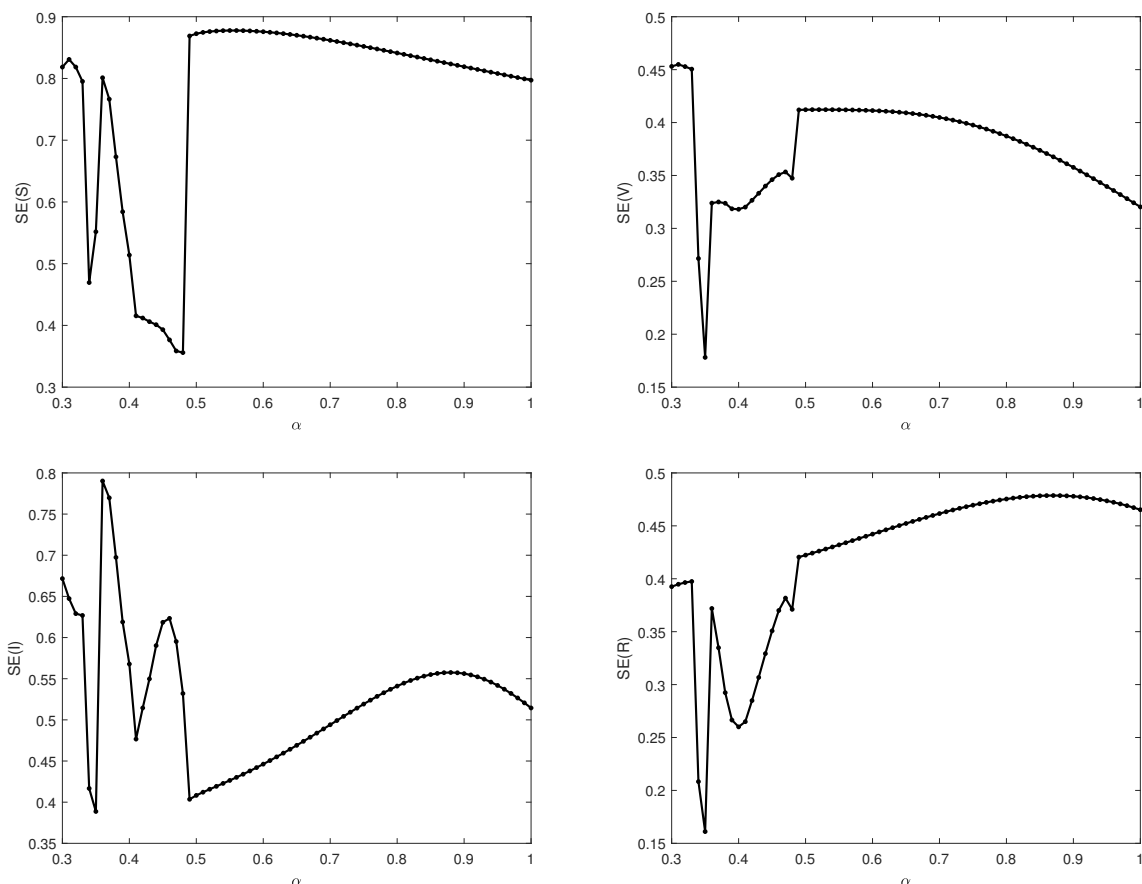


Fig. 5 SE complexity of the state variables on the fractional order.

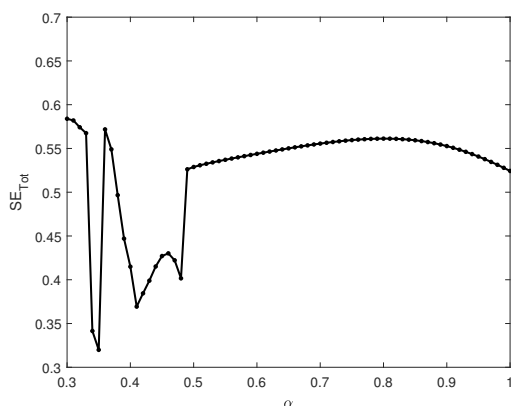


Fig. 6 SE_{Tot} complexity of the system (1) on the fractional order.

it gives us useful information by the SE analysis that the fractional system (1) has different dynamic behaviors when the order across the critical value of $\alpha^* = 0.5$.

CONCLUSION

The order of the fractional derivatives in a fractional-order system is a key parameter with significant effects on solution and dynamics of the system. However, the dynamics of a fractional-order differential system seems to have no relations with the order of the fractional derivative if utilizing traditional analysis methods. This work has made an exploration to reveal the relation between the oscillatory bifurcations and the fractional orders by employing the spectral entropy complexity of the orders. This methodology can be generalized to deal with dynamic problems in nonlinear fractional-order differential systems.

We will continue to study the mechanism of SE complexity on the fractional orders with the dynamics of bifurcation, and then consider some inverse problems for the fractional-order SVIRS system, especially the inverse problem of identifying the order of the fractional derivative and the variable-order time fractional model [36] in the near future.

Acknowledgements: This work was supported by NNSF of China (No. 11871313).

REFERENCES

1. Anderson RM, May RM (1979) Population biology of infectious disease. *Nature* **280**, 361–367.
2. Hethcote HW (2000) The mathematics of infectious diseases. *SIAM Rev* **42**, 599–653.
3. Ma ZE, Zhou YC, Wu JH (2009) *Modeling and Dynamics of Infectious Diseases*, CAM 11, Higher Edu Press & World Sci Publishing, Beijing & Singapore.
4. Dokoumetzidis A, Magin R, Macheras P (2010) A commentary on fractionalization of multi-compartment models. *J Pharmacokinet Pharmacodyn* **37**, 203–207.
5. Diethelm K (2013) A fractional calculus based model for the simulation of an outbreak of dengue fever. *Nonlinear Dyn* **71**, 613–619.
6. Gonzalez PG, Arenas AJ, Chen CBM (2014) A fractional order epidemic model for the simulation of outbreaks of influenza A (H1N1). *Math Method Appl Sci* **37**, 2218–2226.
7. Huo JJ, Zhao HY, Zhu LH (2015) The effect of vaccines on backward bifurcation in a fractional order HIV model. *Nonlinear Anal Real World Appl* **26**, 289–305.
8. Kheiri H, Jafari M (2019) Stability analysis of a fractional order model for the HIV/AIDS epidemic in a patchy environment. *J Comput Appl Math* **346**, 323–339.
9. Angstmann CN, Erickson AM, Henry BI, McGann AV, Murray JM, Nichols JA (2017) Fractional order compartment models. *SIAM J Appl Math* **77**, 430–446.
10. Angstmann CN, Erickson AM, Henry BI, McGann AV, Murray JM, Nichols JA (2021) A general framework for fractional order compartment models. *SIAM Rev* **63**, 375–392.
11. Guo ZG, Sun GQ, Wang Z, Jin Z, Li L, Li C (2020) Spatial dynamics of an epidemic model with nonlocal infection. *Appl Math Comput* **377**, 125158.
12. Ahmad S, Ullah A, Al-Mdallal QM, Khan H, Shah K, Khan A (2020) Fractional order mathematical modeling of COVID-19 transmission. *Chaos Soliton Fract* **139**, 110256.
13. Boudaoui A, Moussa YE, Hammouch Z, Ulla S (2021) A fractional-order model describing the dynamics of the novel coronavirus (COVID-19) with nonsingular kernel. *Chaos Soliton Fract* **146**, 110859.
14. Ghorri MB, Naik PA, Zu J, Eskandari Z, Naik M (2022) Global dynamics and bifurcation analysis of a fractional-order SEIR epidemic model with saturation incidence rate. *Math Method Appl Sci* **45**, 3665–3688.
15. Higazy M (2020) Novel fractional order SIDARTHE mathematical model of COVID-19 pandemic. *Chaos Soliton Fract* **138**, 110007.
16. Pandey P, Chu YM, Gomez-Aguilar JF, Jahanshahi, H (2021) A novel fractional mathematical model of COVID-19 epidemic considering quarantine and latent time. *Result Phys* **26**, 104286.
17. Lu ZZ, Ren GJ, Chen YQ, Meng XY, Yu YG (2023) A class of anomalous diffusion epidemic models based on CTRW and distributed delay. *Int J Biomath* **16**, 2250130.
18. Wu ZH, Cai YL, Wang ZM, Wang WM (2023) Global stability of a fractional order SIS epidemic model. *J Differ Equ* **352**, 221–248.
19. Wang Z, Li GS (2025) Complexity and chaos of a time-fractional SAIR epidemic system with respect to fractional order. *Phys Scr* **100**, 075234.
20. Nisar KS, Farman M, Abdel-Aty M, Ravichandran C (2024) A review of fractional order epidemic models for life sciences problems: Past, present and future. *Alex Eng J* **95**, 283–305.
21. Goel K, Kumar A, Nilam (2020) A deterministic time-delayed SVIRS epidemic model with incidences and saturated treatment. *J Eng Math* **121**, 19–38.
22. Yang B, Yu ZH, Cai YL (2022) The impact of vaccination on the spread of COVID-19: Studying by a mathematical model. *Phys A Stat Mech Appl* **590**, 126717.
23. Podlubny I (1999) *Fractional Differential Equations*, Academic Press, NY.
24. Castillo CC, Song B (2004) Dynamical models of tuberculosis and their applications. *Math Biosci Eng* **1**, 361–404.
25. Costa M, Goldberger AL, Peng CK (2002) Multi-scale entropy analysis of complex physiologic time series. *Phys Rev Lett* **89**, 068102.
26. Staniczenko PPA, Lee CF, Jones NS (2009) Rapidly detecting disorder in rhythmic biological signals: A spectral entropy measure to identify cardiac arrhythmias. *Phys Rev E* **79**, 011915.
27. Klein JT, Karpov EG (2021) Spectral entropy and strain energy trends in composite mechanical metamaterials. *Extreme Mech Lett* **45**, 101289.
28. Yan MX, Liu XD, Jie JF, Hong Y (2024) Construction and implementation of wide range parameter switchable chaotic system. *Sci Rep* **14**, 4059.
29. Anatoly AA (2015) A new difference scheme for the time fractional diffusion equation. *J Comput Phys* **280**, 424–438.
30. Luo WH, Huang TZ, Wu GC, Gu XM (2016) Quadratic spline collocation method for the time fractional subdiffusion equation. *Appl Math Comput* **276**, 252–265.
31. Zhao YL, Gu XM, Ostermann A (2021) A preconditioning technique for an all-at-once system from Volterra subdiffusion equations with graded time steps. *J Sci Comput* **88**, 11.
32. Zhou JF, Gu XM, Zhao YL, Hu L (2015) A fast compact difference scheme with unequal time-steps for the tempered time-fractional Black-Scholes model. *Int J Comput Math* **101**, 989–1011.
33. Adomian G (1984) A new approach to nonlinear partial differential equations. *J Math Anal Appl* **102**, 420–434.
34. Bhalekar S, Daftardar-Gejji V (2011) A predictor-corrector scheme for solving nonlinear delay differential equations of fractional order. *J Fract Calc Appl* **1**, 1–9.
35. Kai D, Ford NJ, Freed AD (2002) A predictor-corrector approach for the numerical solution of fractional differential equations. *Nonlinear Dyn* **29**, 3–22.
36. Gu XM, Sun HW, Zhao YL, Zheng XC (2021) An implicit difference scheme for time-fractional diffusion equations with a time-invariant type variable order. *Appl Math Lett* **120**, 107270.